Organic Multilayer Photoconductor Utilizing a Spacer Layer

by

Jill A. Rowehl

Submitted to the Department of Materials Science and Engineering
in Partial Fulfillment of the Requirements for the Degree of

Bachelor of Science

at the

Massachusetts Institute of Technology

June 2008

Signature of Author.....
Department of Materials Science and Engineering
May 6, 2008

Certified by .....
Vladimir Bulović
Associate Professor
Thesis Supervisor

Accepted by .....
Caroline A. Ross
Chair, Undergraduate Committee

Organic Multilayer Photoconductor Utilizing a Spacer Layer

by Jill A. Rowehl

Submitted to the Department of Materials Science and Engineering
May 6th, 2008
In Partial Fulfillment of the Requirements for the Degree of
Bachelor of Science in Materials Science and Engineering

ABSTRACT

Chemosensors hold many vital applications in today's world, particularly as detectors for explosives. There is still vast room for improvement as other technologies—particularly those of explosives—continue to evolve and expand. Herein, we develop a novel device structure with the potential for much higher sensitivity. The lateral bilayer photoconductor is comprised of an exciton generation layer (EGL) and a charge transport layer (CTL). This separates the functionality of chemical sensing from the charge transport, allowing each film to be independently optimized. As a further improvement on this structure, we introduce a spacer layer to separate charge carriers in the EGL and the CTL, reducing bimolecular recombination at the interface.

As a proof of concept, we fabricate and characterize lateral multilayer photoconductors composed of small molecule organic films. It is experimentally demonstrated that the utilization of a spacer layer can produce an order of magnitude enhancement in quantum efficiency over the bilayer device. The possible mechanisms causing this enhancement are described and examined. The work reported here provides encouraging results in the fields of chemosensors and organic optoelectronics.

Thesis Supervisor: Vladimir Bulovic
Title: Associate Professor of Electrical Engineering and Computer Science

ACKNOWLEDGEMENTS

There are many, many people whom I should thank for assisting me through my thesis, my research, and most importantly through life.
I am greatly indebted to John Ho, my grad student and mentor. The one who unexpectedly agreed to take me on as a UROP one and a half years ago and who has patiently taught me ever since. From him I have learned a lot about photoconductors and chemosensors, depositing organic films and characterizing devices, plotting data and bolting stainless steel parts together. I've also learned a lot about research, about trying new things, pursuing what looks interesting and broadening my knowledge. Further, I've experienced excessive patience and understanding and witnessed great devotion. John is my new definition of hardcore ☺ I can't thank John enough, and I surely can't thank God enough for placing John in my life.
To my advisor, Vladimir, who also took me in when I randomly showed up at his door and begged to work on OLEDs with him. He has always welcomed me into his office to answer my questions, and he has always had the most delicious candy to offer. I have searched the nation over and decided that he is the best boss for me. I greatly appreciate the opportunity to continue in his group. I can only look forward to the many things that I will learn from and with him over the next few years.

I am grateful for every member of LOOE (including the Soft Semi group ☺). I appreciate the random, unexpected questions (and lessons) at group meetings, the random lessons on how to use/fix various lab equipment, and the random, impromptu discussions on their research. As above, I've searched the nation over and decided that this is the very best group for me. I'm exceedingly glad to be staying here.

The following people aren't necessarily listed by importance, but rather in the order that I remember them at 1am.
Alexi, who taught me numerous aspects of Courses 6 and 8, has convinced me the photons are pretty cool, and has nearly convinced me that solar cells are fun to research ☺ And who has given me the concept "being like Alexi" = knowing the lab equipment as well as he does. I undoubtedly have much more to learn from him.
Tim, who always makes me laugh when I think of him. Who has learned along with me and yet is also someone of whom I can ask for help and guidance. I'm grateful that you're not graduating anytime soon. ^_^
Conor, who has given me an enormous goal for my grad school years. I have taken over his desk determined to eventually know as much as he did about organic optoelectronics. Hopefully some day I will be as useful in explaining theories to some UROP student as he was to me. Thanks for befriending the young UROP who was forced into your office ☺
Jen, who makes me smile and who gives me really yummy cookies =D Who gets me away from my desk to eat lunch and who ensures that we have the most awesomest lab in the world.
LeeAnn, my officemate for the longest 6 months ever, of whom I enjoyed her presence and conversation greatly and whom I love to tell other people about (I shared a desk with a farmer!).
Scott, who knows more about optics than I could ever know and who has patiently tried to teach it all to me, and who has allowed me to happily open many packages of paper, pens, and binder clips.

Ivan, who provided me with substrates for a very long time, and who taught me how to put on a bunny suit and showed me what he does while wearing it (read the sports news online ;-). Clearly, I can't list everyone, but THANK YOU all.

There are several people whom have been with me throughout my undergrad years. Forgive me for being brief:
Craig: who paid me, signed my forms, and continually gave me great advice even when I didn't take it.
Jung Yoon: who has seen me as me and yet still loves me. Tiffany, Tami: for living with me and putting up with me for 4+ years. Pastor Paul, Becky JDSN, David JDSN, Angela SMN: my leaders and teachers. Donald, James, Austin, Justin, Orton, Etak, Doug: my dear oppas. Susie, Jenny, Joanne, Helen: my older sisters in Christ. Brandon and Seng, my peers and co-workers. My younger sisters and brothers in Christ who are so encouraging. Including Anna, for whom I cannot praise God enough.
For ABSK—through whom my life was saved—I cannot thank God enough.

Thanks to my family: my mother and father who brought me up, supported me, and taught me to always try my best. My older sister, Deb, who put up with me. My younger sister, Pam, who I learned to put up with. Grandma and Dad, who have supported me in all things. And the rest of my family: much too long to list. You have all shaped me into who I have become.

Finally, I thank God, who made it so simple: He loves me. Not only did He *give* me life, but He has given me life *in abundance*. He called me to grad school and sent me to Vladimir's door. He has proven time and time again that He will provide. And now, I completely trust in His promise.

"For I know the plans I have for you," declares the LORD, "plans to prosper you and not to harm you, plans to give you hope and a future."
-- Jeremiah 29:11

PREFACE

There is a story to my undergrad thesis research, and as much as I wanted to tell it elsewhere, John persuaded me that it simply does not belong in a formal, scientific thesis report. However I compromised: so here's my preface ^_^

Once upon a time, John Ho (my mentor) and Prof. Vladimir Bulović (my thesis advisor) began to explore a possible device structure, the lateral heterojunction. This device will (hopefully) be useful as a chemosensor, specifically for TNT and DNT: fearful molecules to many men. However, there was (and still is) much to explore and understand about this novel device structure. The story advances: one day I appeared at Vladimir's office requesting to work on organic optoelectronics with him, and my role became to explore one method of possibly improving said device structure.

However, my research has become more than just optimizing a device. Through the I-V curves, the QE data, the AFM images, the response to annealing… and even through simply looking at the energy band diagrams really hard, I –and we—have learned a lot about this device structure and about organic interfaces, particularly between the organic materials of interest in this research. When a device is composed of two materials rather than just one (or, as in this work, three materials rather than just two), its behavior is not simply the superposition of the behavior of isolated materials. Nor can we simply assume that the isolated behavior of one of the materials will always be the behavior of the multilayer device. Both materials affect the other—and possibly drastically— at their interface, and we have found that this device structure (the lateral multilayer photoconductor) gives us a wondrous opportunity to explore those effects.

And that is what this work is about. In these pages I have attempted to record all that I have learned over the past year: excitons, traps, device physics. This is for my own benefit: both to learn through writing it as well as to have a record of my knowledge so that I may look back upon it later. It is also for the benefit of others, however (as is all proper scientific research), and thus I have attempted to make it as clear and professional as possible (with John's assistance).

So please enjoy, and please learn. This thesis is a record of a massive chunk of one year in my life and a foundation for several more. I pray that others may benefit from it.

TABLE OF CONTENTS

LIST OF FIGURES

LIST OF TABLES

CHAPTER 1: INTRODUCTION

Chemosensors[1] are becoming more and more useful for everyday life and often require advanced technology for optimal performance. These devices are being developed in many fields and from many directions: two examples from recent headlines out of MIT are from Prof. Thomas' group in the Department of Materials Science and Engineering using photonic block co-polymers to sense environmental parameters such as humidity and salinity[i] and from Prof. Akinwande's group in the Department of Electrical Engineering and Computer Science using gas chromatography and mass spectrometry to detect hazardous gases[ii]. However, there is continual need for improvement, especially for higher and higher sensitivities of explosives sensors. The most sensitive device in the field of TNT detectors is Fido™, manufactured by ICx-Nomadics. A novel device structure, the lateral multilayer photoconductor, is currently being developed with potential for improved sensitivity over Fido™. In this work, we investigate a lateral trilayer photoconductor and explore possible mechanisms of the photogenerated current and, correspondingly, the sensitivity of the device.

State-of-the-Art Chemosensors and Their Limitations

Fido™

Fido™—initially developed by Tim Swager's group (in the Department of Chemistry at MIT), commercially distributed by ICx-Nomadics and employed in the field by the U.S. armed forces—utilizes the fluorescence signature of polymers to transduce a chemical signal of TNT or DNT into an electrical signal. In ambient atmosphere, the polymer will fluoresce when excited by UV light. However, the presence of explosives introduces a mid-gap state which allows an

[1] A chemosensor is a device that transduces the presence of a chemical species into a more easily quantifiable signal, such as current or light. Chemosensors can be designed to detect a specific analyte (a chemical species) or designed to determine the type of chemical species present in the environment.

excited electron to relax without emitting light. Thus the polymer emission will "turn off"[iii], giving an optical signal which can be measured with a photodetector and transduced into an electrical signal.

Unfortunately, Fido™ is limited by the fact that the transduction mechanism is a two-step process. First, the chemical reaction generates the optical signal, which is then converted into an electrical signal by a photodetector. That electrical signal is analyzed to determine the presence of the analyte. Therefore, one way to improve upon this chemosensor is to directly generate an electrical signal, eliminating the losses inherent in the multiple step transduction mechanism. The lateral bilayer photoconductor is under development as a device that can generate an electrical signal from the chemisorption of an analyte molecule onto the polymer.

Lateral Bilayer Photoconductor

The creation of a sensor that directly generates an electrical signal is not a novel idea, as chemiresistors using interdigitated electrodes have been used for decades to measure everything from moisture levels[iv] to biological molecules[v] to chemical species[vi]. However, the combination of a sensing fluorescent polymer and a photoconductor device architecture forms a device with a chemically modulated, amplified electrical signal. This concept is being developed in our group as the lateral multilayer photoconductor[vii], shown in Figure 1.

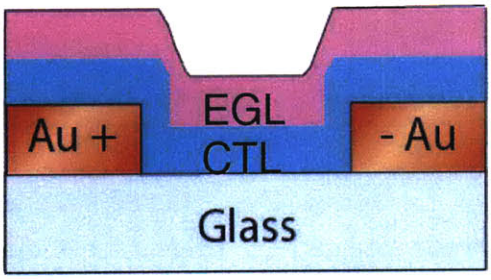

Figure 1 Structure of a bi-layer lateral heterojunction. The gold contacts on either side apply an electric field parallel to the organic interface.

The device structure of the lateral bilayer photoconductor is accomplished by sequentially depositing two semiconducting films onto an array of interdigitated gold electrodes. The top semiconducting film is the exciton generation layer (EGL). The purpose of the EGL is to generate excitons when exposed to light. This layer can be engineered to interact with a specific analyte such that the analyte will quench excitons, i.e. the device will "turn off" in the presence of the analyte. The bottom semiconducting film, which contacts the electrodes, is the charge transport layer (CTL). The purposes of the CTL are (1) to provide an interface for exciton separation and (2) to transport generated charge carriers to an electrode. Utilization of an EGL and a CTL offers the capability of choosing the proper sensing material to mate with a material that has optimal charge carrier mobility.

Operation of the device depends on both the generation of excitons in the EGL and the conduction of charge carriers through the CTL. First, molecules in the EGL are preferentially photoexcited to generate excitons. The excitons diffuse throughout, some finding the interface between the EGL and CTL. At the interface, the excitons generated in the EGL dissociate as one charge carrier is swept to a lower-energy state on a molecule in the CTL. The holes and electrons then drift parallel to the interface under the force of the applied electric field, producing the measured photocurrent.

An internal process that decreases the efficiency of this device is interfacial recombination. The photogenerated charge increases the charge concentration at the interface, but due to Coulombic attraction, charges may recombine across the interface, limiting the steady-state photocurrent. The ratio of the photocurrent over the dark current determines the sensitivity of the device, thus any enhancement of photocurrent with a constant dark current correlates with

an enhancement of sensitivity. In this work, we describe and characterize a possible method of reducing the recombination rate and therefore enhancing sensitivity: utilization of a spacer layer in the lateral multilayer photoconductor.

Objective: Enhancement of Photocurrent via Utilization of a Spacer Layer

The magnitude of the photocurrent has large repercussions on the performance of the potential chemosensor and thus must be maximized. One mechanism of enhancing photocurrent is the utilization of a spacer layer. When the spacer layer forms a cascading energy structure with the CTL and EGL, excitons dissociate at the interface between the EGL and the spacer layer and one of the charge carriers is swept through the spacer layer to a lower energy state in the CTL: the photogenerated charge carriers are distanced from each other. This decreases the Coulombic forces between them and thus decreases the recombination rate. A reduced recombination rate corresponds to an enhanced photocurrent, allowing for a greater response to the presence of an analyte and a corresponding improvement in the sensitivity of the device.

Following this model of optoelectrical behavior, we examine a lateral trilayer photoconductor, shown in Figure 2. As a proof-of-concept, the device is fabricated comprising of small molecule organic semiconducting materials. The three organic semiconducting layers (TPD, Alq3, and PTCBI) form interfaces in parallel to the applied field, thus charge transport is along the interface. TPD is well-researched as a hole-transport material and accordingly is used as the charge transport layer, CTL. Alq3 is well-suited for use as a spacer layer for these two materials because of its energy levels which form a cascading energy structure with TPD and PTCBI. PTCBI is extremely absorptive and accordingly is used as the exciton generation layer, EGL.

Herein I report characterizations of this device and its optoelectrical behavior.

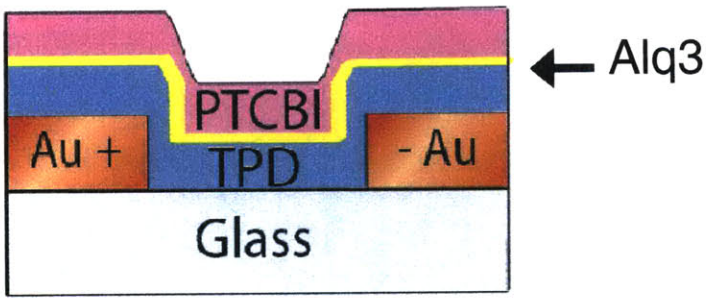

Figure 2 Device structure of the lateral trilayer photoconductor.

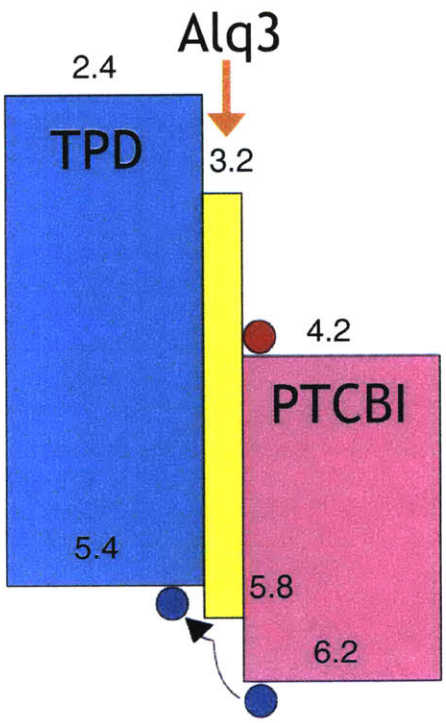

Figure 3 Energy band structure of the trilayer heterojunction. The materials TPD, Alq3, and PTCBI provide a cascading energy band structure for charge carrier drift across interfaces.

Thesis Organization

I have divided my work into four sections:

1. characterization of the materials of interest,
2. background on the optoelectrical behavior of organic multilayer photoconductors,
3. characterization of lateral organic multilayer photoconductors,

   and
4. conclusions and recommendations for further work.

I begin with characterizations of each organic material of interest in order to better understand their combination in a lateral multilayer photoconductor. I then provide some background on the optoelectrical behavior of small-molecule organics and some organic electronic devices. Further, I examine and identify the optoelectrical behavior of lateral organic multilayer photoconductors including the utilization of a spacer layer. Finally, I offer my conclusions and recommend further research to advance our understanding of the lateral organic multilayer photoconductor.

CHAPTER 2: MATERIALS CHARACTERIZATION

There are 4 requirements for our materials choice: 1) a smooth and uniform bulk film and interface, 2) the ability to preferentially excite the EGL, 3) optimal conductivity of the CTL, and 4) an energetic cascade. As discussed below, the choice of TPD as the CTL, Alq3 as the spacer layer and PTCBI as the EGL fulfill these requirements.

Materials of Interest

Here we briefly present a condensed table of the materials properties for TPD, Alq3, and PTCBI. Below we elaborate on the abilities of these three materials to fulfill the requirements for our device.

Table 1: Properties of the Materials of Interest: TPD, Alq3, and PTCBI

Name	HOMO (eV)	LUMO (eV)	Absorption Peak in UV-Vis (nm)	Mobility (cm^2/V-s)
TPD	5.4	2.4	360	10^{-3} (hole)
Alq3	5.8	3.2	400	10^{-8} (hole)
PTCBI	6.2	4.2	532	10^{-6} (electron)

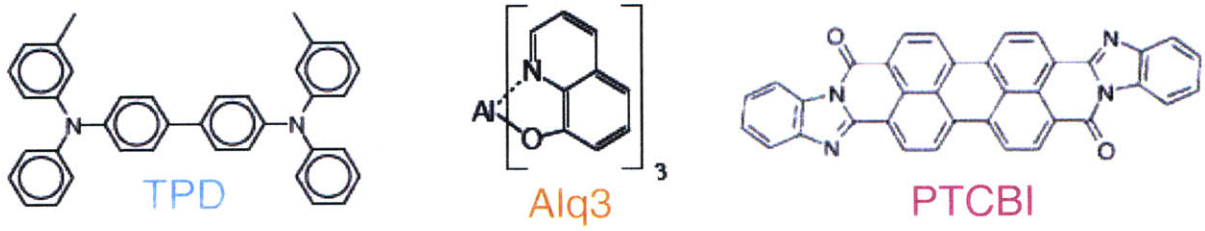

Figure 4 Chemical Structures of Organic Materials of Interest. Shown (left to right) are chemical structures for N,N'-diphenyl-N,N'-bis(3-methylphenyl)-(1,1'-biphenyl)-4,4'-diamine (TPD),aluminum tris-(8-hydroxyquinoline) (AlQ3), and 3,4,9,10-perylenetetracarboxylic-bis-benzimidazole (PTCBI).

A. Morphology

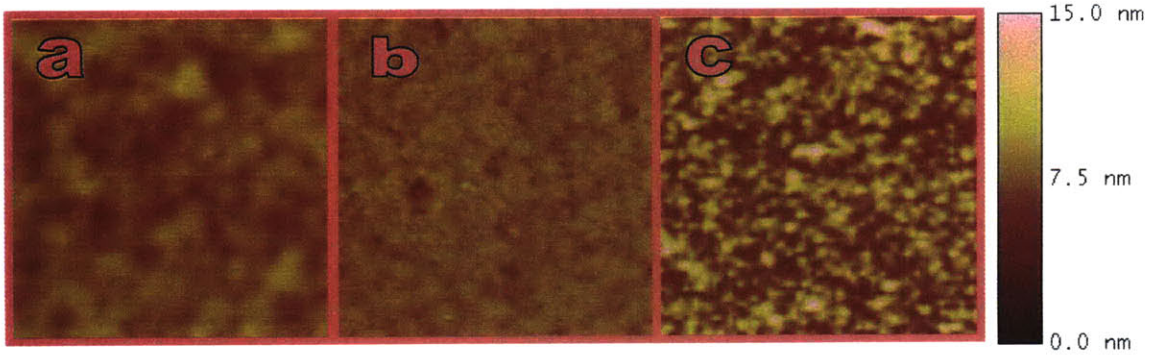

Figure 5 AFM Images of the materials of interest. Shown are **a** glass/TPD 50nm, **b** glass/Alq3 50nm, and **c** glass/PTCBI 50nm. Each image is 1micron across and with a z-scale of 15nm.

All three of these materials form amorphous layers when deposited via thermal evaporation in high vacuum ($<10^{-7}$ Torr) onto glass substrates with no surface treatment. Images from Atomic Force Microscopy (AFM) are shown in Figure 5. The RMS roughness of 50nm films of Alq3, TPD, and PTCBI are all on the order of nanometers, with TPD and Alq3 exhibiting roughness smoother than that of the glass substrate.

However, the roughness of the organic layer depends greatly on the surface upon which it is deposited. Initially, we used a self-assembled monolayer (SAM) to passify excited states on the glass substrate, which may form traps that create hysteresis in our device current-voltage characteristics. However I found that TPD often balled up on the particular SAM that we were using, causing inconsistency in the device characteristics. For this reason, I stopped using that particular SAM and worked only with clean substrates of glass and photolithographically-patterned gold fingers. Identification of a proper SAM for use with TPD is left for future experimentation.

I present an AFM image of the TPD/Alq3/PTCBI trilayer in Figure 6. It is clear that all three layers are compatible and the result is a smooth, amorphous film. Unfortunately, there is no method of determining the interfacial roughness through simple AFM, however there are procedures to prepare a sample for imaging of the interface, and this as well is left for future experimentation. Nonetheless, we assume that the as-deposited films form an approximately flat interface, since all three layers are individually very smooth as well as the trilayer surface.

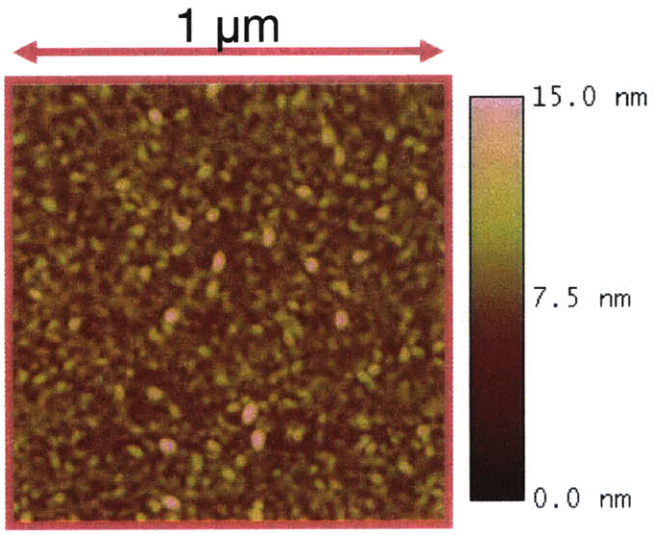

Figure 6 AFM image of the surface of the trilayer: TPD/Alq3/PTCBI. The roughness is on the order of nanometers.

B. Absorption

As the device structure of interest is in the simplest sense a photodetector, it is important to understand the photoresponse of each individual material of interest.

Mechanisms of Absorption

Most importantly, we acknowledge that bulk materials do not respond to a single wavelength, but rather a broad range. In amorphous organic materials, the absorption spectrum of a specific material is determined by four factors: placement of energy bands, probability of transfer between energy bands, vibronic interactions between atoms, and molecular disorder.

Without attempting an in depth discussion of atomic and molecular orbitals, there are general conclusions that can be drawn about the placement of energy bands. The overlap between the energy states at each atom (which is determined by the atomic number and the bonding) determines the energy bands of the molecule as a whole. Also, the size of the molecule (how many atoms are bonded together) determines the placement of the energy bands. As the size of the molecule increases, the electrons are less and less constrained, and thus the distance between energy bands decreases in energy (similarly, the absorption occurs at longer wavelengths) as shown in Figure 7. Thus, each molecule has specific wavelengths (or wavelength ranges) which they will absorb.

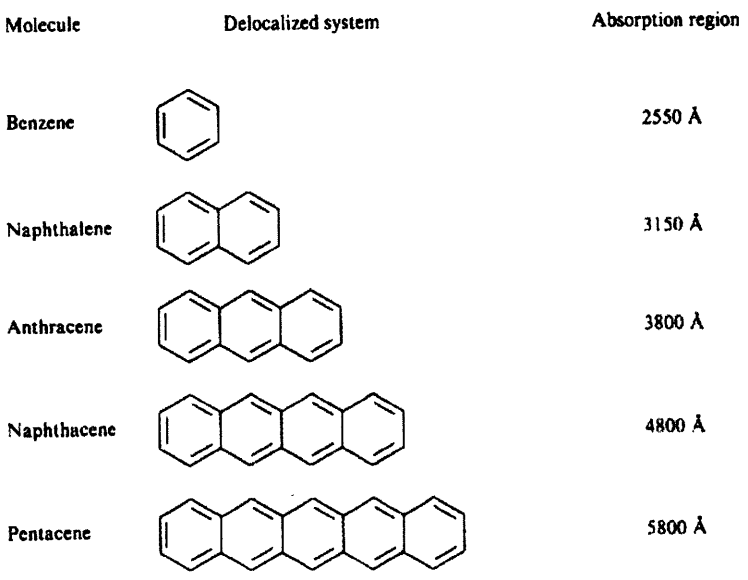

Figure 7 Molecular structures and the wavelength of the main absorption peak for several polyacenes. (Reproduced from Pope[viii].) This demonstrates that as the molecular size increases, the absorption spectrum is red-shifted (to lower energy).

The probability of absorption at each of these available wavelengths is determined by the probability of transfer between energy bands. Thus, each peak in absorption may not have the same intensity; rather they vary depending on the energetics of each energy state.

There are two factors that broaden the absorption peaks: vibrations of the atoms and disorder in the bulk. As the atoms vibrate, the bond lengths vary, broadening the energy bands and thus broadening the absorption spectrum. Also, disorder in the material means that each molecule interacts differently with other molecules and thus has slightly different energy states.

Thus, an absorption spectrum can be very broad or very narrow, may be shifted to high or low energies, or can have different intensities at different wavelengths, depending on many factors. However, for a specific material with an unchanging morphology, we can assume that the absorption spectrum will be roughly constant (as I have seen experimentally as well).

Absorption of Materials of Interest

In Figure 8 I show the absorption spectrums of each material of interest as well as that of the glass substrate. Each spectrum is for a 50nm film of each individual material on a glass substrate. As shown clearly, neither the TPD nor the Alq3 absorb in the green, the main absorption peak of PTCBI. Thus the second requirement for our materials set, the ability to preferentially excite the EGL, is fulfilled.

It is also useful to note that Alq3 is much less absorptive than either TPD or PTCBI in the UV-Vis range, and thus should generate a lower concentration of excitons per intensity of light.

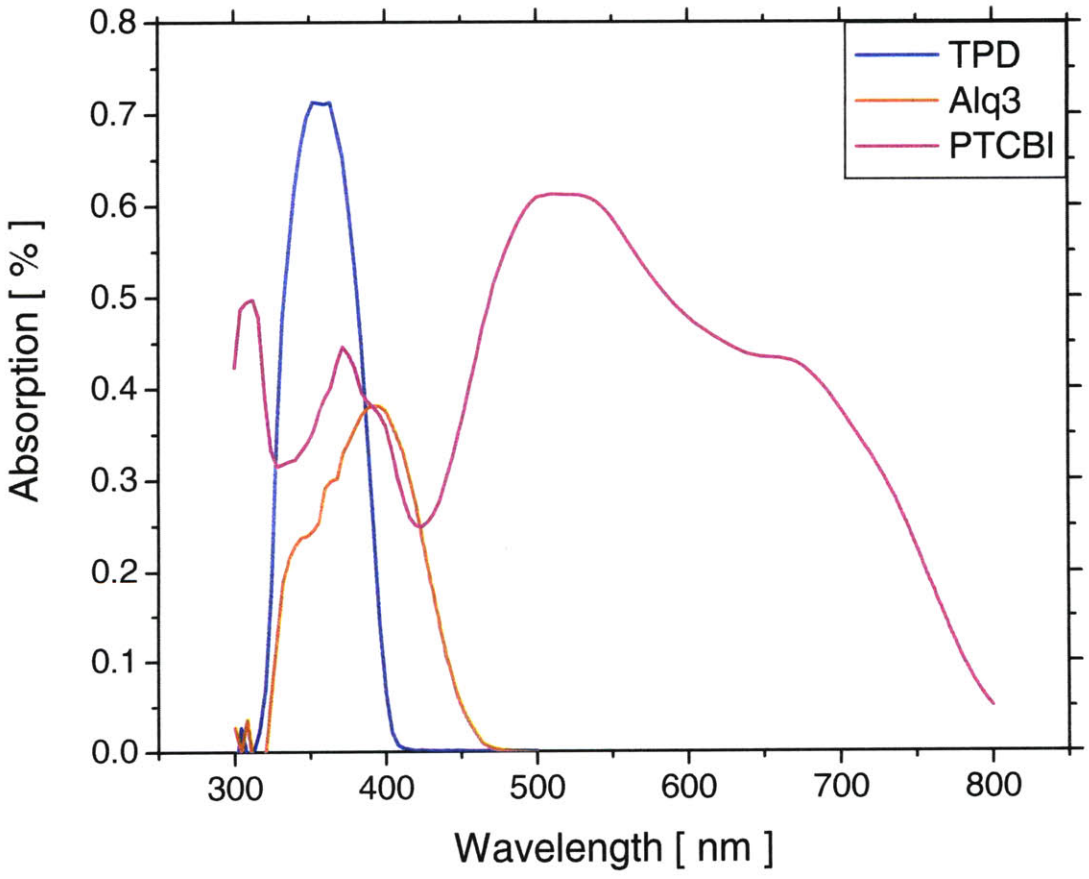

Figure 8 Absorption spectra of the organic materials of interest. Most notably, the PTCBI peak in absorption at approximately 540nm does not overlap with either TPD or Alq3.

C. Conductivity

The third requirement for our materials set is that the CTL conducts charge carriers. TPD has been well-researched as a hole transport material, particularly in organic LEDs. Published values for the hole mobility of TPD are on the order of 10^{-3} $cm^2/V\text{-}s$[ix] (notably very low as compared to the electron mobility of doped Silicon, 10^3 $cm^2/V\text{-}s$[x]). Also, TPD has been shown to have a low concentration of traps, as well as a small electric field dependence[ix].

It is good to also note the electrical behavior of our two other materials: Alq3 and PTCBI. PTCBI has an electron mobility of 2×10^{-6} $cm^2/V\text{-}s$[xi], orders of magnitude below the hole of mobility of TPD. Thus we assume that conduction occurs primarily through TPD.

Alq3 also has an electron mobility on the order of 10^{-6} $cm^2/V\text{-}s$, however its hole mobility is two orders of magnitude lower[ix],[xii]. Therefore we can be sure that the Alq3 won't be the primary channel of conduction laterally. Also, we note that Alq3 exhibits a high concentration of traps for electrons whereas the holes have very few.

D. Energy Levels

In this research, I experiment with materials that form a cascading energy structure (the HOMO and LUMO of the spacer layer are between the HOMO bands and LUMO bands of the EGL and CTL, respectively). With this energy band structure, it will be energetically favorable for one type of charge carrier to hop to molecules in the CTL and the opposite type to remain in the EGL.

Previously we have found high efficiencies with the bi-layer heterostructure constructed of TPD (HOMO = 5.4 eV, LUMO = 2.4 eV) as the CTL and PTCBI (HOMO = 6.2 eV, LUMO = 4.2 eV) as the EGL. An ideal spacer layer for this structure is tris-(8-hydroxyquinoline)

aluminum (Alq3, HOMO = 5.8 eV, LUMO = 3.2 eV), which forms a cascading energy structure (see Figure 3). Thus this work includes research on TPD, Alq3, and PTCBI[2].

[2] There are other materials that can be used as a spacer layer with TPD and PTCBI. This future research is discussed in Chapter 6.D.

CHAPTER 3: BACKGROUND ON OPTOELECTRONICS

An understanding of the individual materials is vastly important; however our purpose is to make use of the interaction between the materials. The ultimate goal of this device is to transduce a chemical signal into an electrical signal, and thus we must study the optoelectrical behavior of the device.

A. Small Molecule Organic Optoelectronics

Any background on organic optoelectronics wouldn't be complete without citing Tang and VanSlyke[xiii], the key example for OLEDs (organic light emitting diodes). In 1987, Tang and VanSlyke were the first to demonstrate a viable organic electroluminescent diode with a high efficiency and a low operating voltage. Their device, reproduced in Figure 9, comprised of a vertically-biased heterojunction of Alq3 and an aromatic diamine (similar to TPD). Their research set off an incredible expansion of OLED research, culminating to a potentially billion dollar international industry, which we are right in the middle of watching it take off[3]. These same materials are the ones that I have chosen to explore in my thesis research.

[3] Sony recently introduced the first commercially-available OLED TV http://ces.cnet.com/8301-13855_1-9842035-67.html

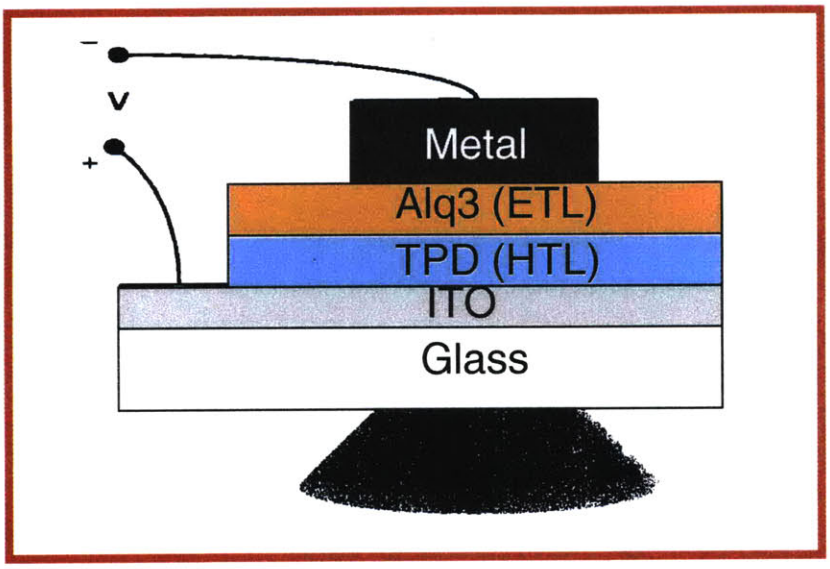

Figure 9 OLED structure.

Excitons and Polarons: Formation and Termination

First and foremost, a strong foundation in polarons and excitons—charge carriers in small-molecule organics—is necessary to understand electrical behavior in these devices. Cartoon images of both polarons and excitons are shown in Figure 10.

Polarons are the negative and positive charge carriers in small-molecule organic devices. A negative polaron is the addition of an electron to an excited state in an already-filled molecule. The extra electron gives a negative charge to the molecule. A positive polaron is the subtraction of an electron from an already-filled molecule. The missing electron gives a positive charge to the molecule. In this work, negative polarons will be simply identified as "electrons" and positive polarons will be identified as "holes".

Excitons, however, are a neutral combination of a negative polaron and a positive polaron: there is an extra electron in an excited state and a missing electron in the ground state. Because of this, it is both an excited state (and thus requires an input of energy to be generated),

yet is also neutral and unaffected by electric fields[4][xiv]. Excitons can be generated with either spin 0 or spin 1, as shown in Figure 10, which can have vast effects on OLEDs. However this research is virtually unaffected by the difference between the two and thus spin will be ignored.

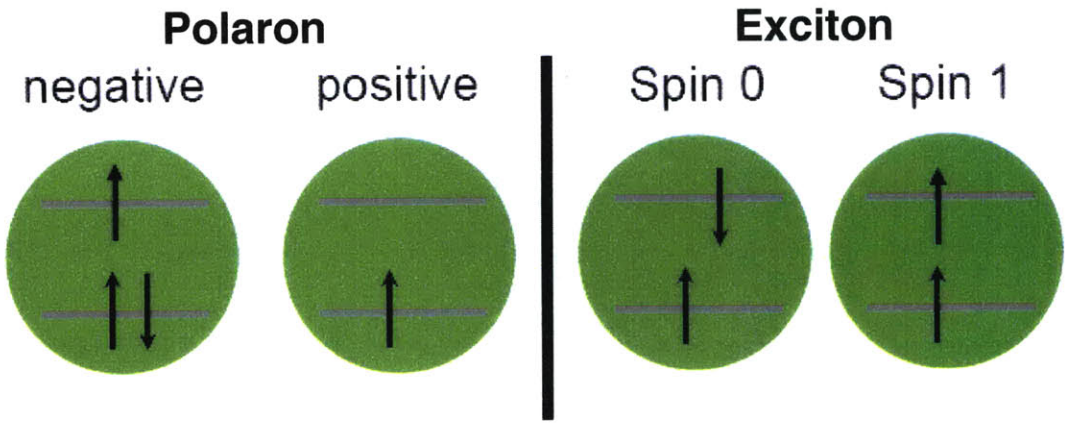

Figure 10 Cartoons showing Polaron and Exciton energy level structures. Polarons are not simply electrons and missing electrons but rather depend on filling specific molecular orbitals. Excitons are an excited, yet electrically neutral state. (Diagram reproduced from Madigan[xv]).

Mechanisms of exciton formation and termination

The generation of excitons is where optics comes into play. Above, I discussed the absorption of a material with no mention of the word "excitons". However, we did explore the excitation of electrons, which is essentially an exciton.

My first question when I came upon excitons in organic materials was "why don't these things exist in inorganics?" The answer is: they do, but they disassociate into holes into electrons far easier than in organics. They're binding energy is far smaller and they are much more spread out. Thus, they disassociate very quickly and their influence on the device operation is negligible.

---

[4] Actually, excitons can sometimes be influenced by electric fields since they are very similar to dipoles. At very high fields, an exciton can actually be split and drawn to either electrode. However, in this work we assume that we do not bias with such large electric fields.

Mechanisms of polaron formation and termination

There are three ways for polarons to come into existence within a material: intrinsic generation, injection, and exciton disassociation. Intrinsic carriers are formed with an electron moves to an excited state of another molecule: this creates both a positive and a negative polaron (a hole and an electron). At 0K, there are no intrinsic charge carriers, however with the presence of heat carriers may be generated and exist in steady-state.

Another mechanism of generation is injection. The metal contacts on either side inject charges into an organic material. However, often the workfunction of the contact is not equal to the energy level of the conducting band in the organic, and this may form a barrier to injection. For example, gold has a workfunction of 5.2 eV and the HOMO in TPD (which conducts holes) is at 5.4 eV, thus there is a 0.2 eV barrier for the injection of holes into TPD from a gold contact. This injection barrier is shown in Figure 11.

The final mechanism for polaron formation is the disassociation of excitons.

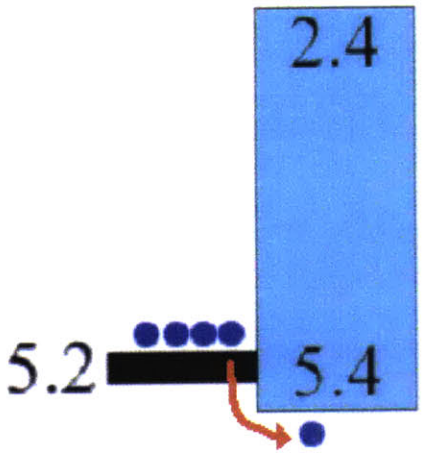

Figure 11 Energy level diagram of the injection barrier between gold and TPD.

Exciton and Polaron: Transport

Both polarons and excitons can move by simple diffusion. This diffusion is from molecule to molecule through the bulk, and thus the energy states of all neighboring molecules must be taken into account. Polarons, however, can also be influenced by an electric field. This doesn't mean that they travel only in one direction, such as in ballistic transport, but rather it means that a polaron has a non-zero average velocity: it's moving in a specific direction.

Polarons move along conjugated bonds and transfer between molecules. Since conjugated bonds are composed of p_z orbitals that are out of the axis of atoms, the electrons often can simply zoom along the molecular backbone and transfer from molecule to molecule.

However each molecule affects the molecular orbitals of its neighboring molecules. Every molecule is a slight dipole, and as such has some affect on the movement of electrons around it (even electrons not in its orbitals). In crystalline materials, every molecule is aligned and thus all of the molecular interactions are the same (excepting the surface molecules). However, we work with amorphous materials, not crystalline. As such, we cannot expect all of the molecular interactions to be the same and thus not all of the molecules have exactly the same energy state. The probability of various interactions between molecules gives rise to a Gaussian distribution of energy states within the bulk material (see Figure 12): some molecules provide lower energy states to conducting carriers and some molecules provide higher energy states to conducting carriers.

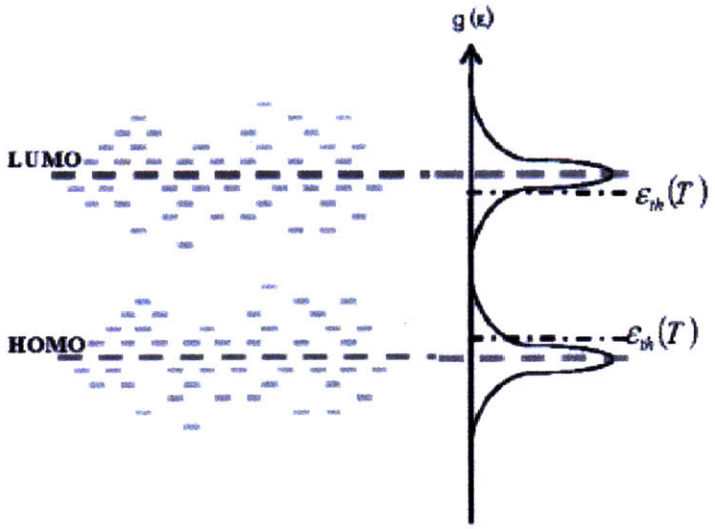

Figure 12 Energetic distribution of states in TPD (traps). The Gaussian distribution of trap-states is made clear on the right-hand side. Reproduced from Shimakawa et al[xvi].

This leads to some complication in charge conduction. The frequency with which a carrier hops from molecule to molecule depends on the difference in energy states between its current state and the possible future state. If the possible state has a lower energy, then the carrier will hop to the lower state. If the possible future state has a higher energy, then it is much less probable that the carrier will hop to the higher state. Thus, a charge carrier will (most probably) move to the lowest state available. But from there, all of the surrounding states are of higher energy and thus there is a low probability (dependent on the energetic barrier) that it will hop to a surrounding state: the carrier is trapped. However, there is still a finite probability, and the carrier will eventually hop out of the state onto a neighboring molecule and continue on its merry way towards one of the electrodes.

In conclusion, it is these trap states that limit the motion of electrons. The longer they are in states, the longer it takes them to reach the opposite electrode. An increase in trap density

entails a decrease in mobility. And a filling of traps entails an increase in mobility. These effects will be discussed below in the device physics section.

B. Laterally-biased Heterojunctions

The interesting part is when these materials and their interfaces are combined with contacts. Often, the heterojunction is biased and probed vertically, as seen in Figure 9. However, further information about the interface can be derived from biasing along the interface. To perform this research, we use substrates with photolithographically-defined gold fingers.

In this section, I expand briefly on the history and behavior of devices utilizing interdigitated contacts. With the geometry of the electric field in mind, I examine photoconductivity as well as the various conduction regimes that a semiconductive device may operate within. Finally, I present former research on the bilayer laterally-biased heterojunction to provide a foundation for understanding the trilayer device.

Interdigitated Gold Electrodes

Arrays of interdigitated metal electrodes have been utilized as device contacts for many decades. They provide a balance between a large area revealed to the environment and a short electrical channel. The large exposed area can be vastly important in the field of sensors: for photodetectors it is necessary to collect as many photons as possible and for chemosensors it is necessary to interact with as many molecules of the analyte as possible. Also, a short electrical channel can be necessary for devices such as organic semiconductors or other materials that are very resistive. An example of interdigitated gold electrodes utilized for both of these purposes is

from Miasik et al.[vi], which designed a chemosensor comprised of a interdigitated gold electrodes connected with a conducting polymer with a conductivity-dependence on the presence of NO_2.

Briefly, our substrates are created through a lift-off process. Photoresist is spun onto a glass substrate and photolithographically-patterned. An initial film of Chromium (20 nm) and then a thick film of Gold (50 nm) are deposited onto the substrate and any metallic film that is deposited on top of photoresist is "lift[ed]-off" during the etching process, producing a substrate with gold electrodes and smooth glass channels. Images of our substrates are shown in Figure 13. Only a portion of the device area is shown in Figure 13a; the total device area is approximately 1.5 mm^2. The AFM image clearly shows an electrode height of 95 nm and demonstrates that the channel is completely clear of gold (the RMS roughness of the channel is 0.6 nm). Channel widths vary between 10 microns and 14 microns from wafer to wafer but are approximately constant within the same region of a wafer. For this reason, devices on different substrates taken from the same wafer are assumed to be of similar geometry.

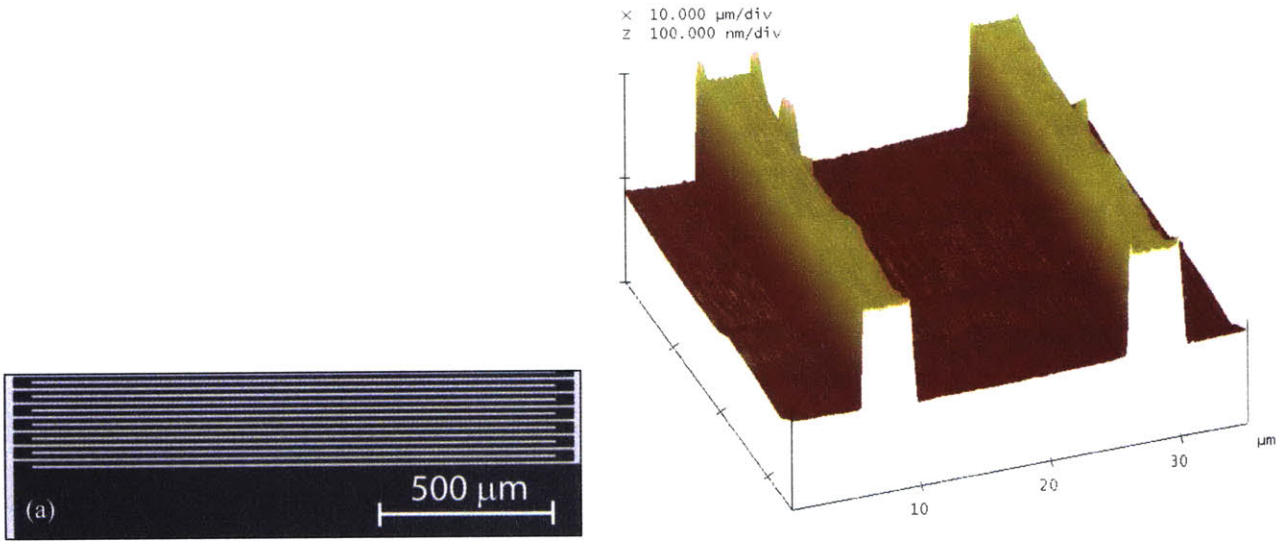

Figure 13 Optical and AFM images of the substrate with interdigitated gold electrodes. **a** Optical microscope image of a portion of the device area. Dark regions are the glass and light regions are the gold electrodes. **b** AFM image of two gold fingers and the glass channel separating them with low resolution.

Photoconductivity

As mentioned above, interdigitated metal fingers are often used in photodetectors due to the large area of semiconductor exposed to light. These devices make use of photoconductivity: the dependence of conductivity on light.

Conductivity is linearly dependent on two factors: the concentration of charge carriers and the mobility of charge carriers through this equation

$$\sigma = q*\mu(n)*n$$

where σ is conductivity, q is the elementary charge, $\mu(n)$ is the mobility with a dependence on n, n is the carrier concentration, and it is assumed that the concentration of majority charge carrier is far greater than that of the minority carrier. As discussed in the background above, photons of specific energies can excite electrons and generate excitons. Even in organic materials, traps exist at which excitons disassociate into polarons, the charge carrier.

Thus, as the intensity of incident light increases, the concentration of charge carriers also increases, linearly increasing the conductivity.

This relationship between conductivity and incident light absorption is demonstrated in Figure 14, where the current through a device is plotted against the applied electric field in both dark and light (a green LED). Focusing on only the PTCBI device (the blue dashed and solid lines), it is clear that exposure to green LED light increases the conductivity of the device by over an order of magnitude. The necessity of exposing the device with the correct wavelength is demonstrated through the TPD device, in which the conductivity is not affected by the green light.

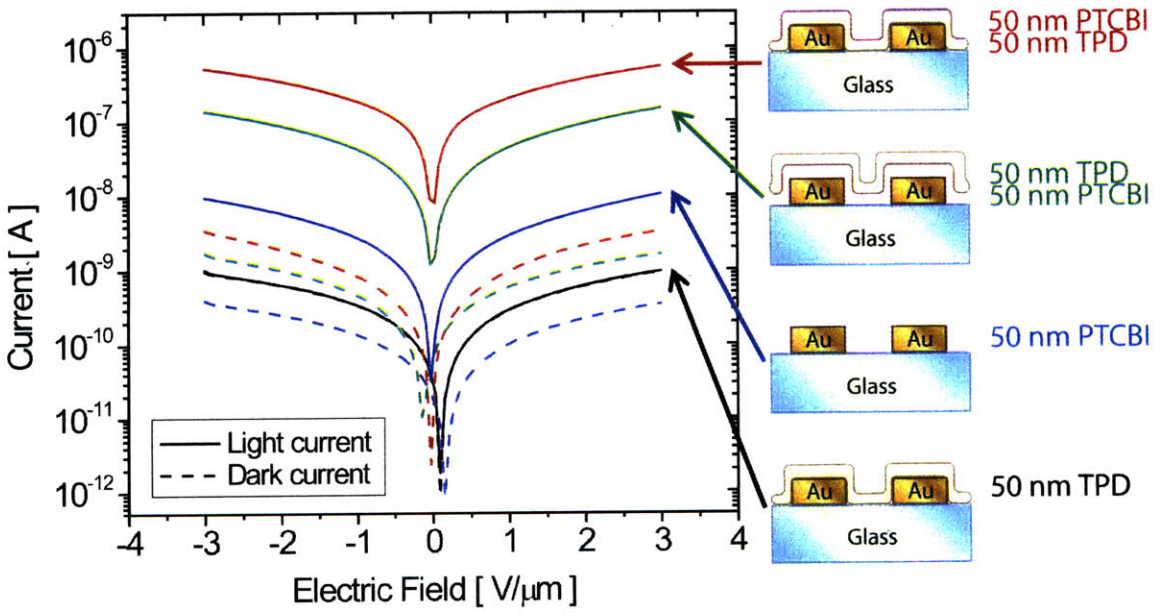

Figure 14 Current-Field Characteristics for various device structures in both dark and light. The benefit of the heterojunction interface is clearly demonstrated in the order of magnitude enhancement of the light current[vii]

However, the relationship is only linear in a certain applied voltage regime: Ohmic Conduction. There are essentially three regimes for an operating, semiconducting device: Ohmic Conduction (OC), Trap Limited Conduction (TLC), and Space-Charge Limited Conduction (SCLC).

Ohmic Conduction (OC)

The regime of Ohmic Conduction is what many of us would expect from a device: the material is resistive, and the conductivity of the material is roughly constant over this regime. As the applied voltage is increased, the current increases linearly. The slope of an I-V curve in this regime is simply equal to 1.

But what is resistance? What is it that is slowing down the electron (or hole, as in the case of TPD) from simple ballistic conduction? In my materials, the limiting mechanism is traps. As mentioned above in the Mechanisms of Polaron Transport section, traps are low energy states from which it is unlikely that an electron will hop out. The more traps there are, the more chances an electron has of falling in, and thus the slower the average velocity (and thus current) will be. Traps are characteristic of a material or of an interface and do not simply disappear when a voltage is applied. However, the effects of traps can be dissipated by the presence of a high concentration of carriers, as is examined below in TLC.

Space-Charge Limited Conduction (SCLC)

At high current densities, the conducting charge carriers themselves create a significant electric field. This charge within the device, known as space-charge, generates a field that counteracts the applied field.

This regime is very similar shielding effect of electrons orbiting an atom on another electron. An electron may be attracted by the nucleus but repulsed by the orbiting electrons. Depending the quantities of charges involved, the extra electron may or may not enter an orbital of the nucleus. Similarly, an extra electron in one electrode may be attracted to the opposite electrode; however there are other electrons between the extra electron and the opposite electrode. Depending on the charge concentration in the semiconductor, the extra electron may or may not transfer into the semiconductor (inject into the device). When the charge concentration is so high as to delay injection, the SCLC regime is reached. Current in the SCLC regime obeys a power-law such that the current density is proportional to the square of the applied voltage[xvii].

Trap Limited Conduction (TLC)

In the TLC regime, the conductivity of the device depends on the applied voltage. As higher voltages are applied to the device, higher and higher quantities of charge carriers are injected into the semiconducting material. These carriers move along, falling into traps and hopping out of traps. But at a certain point, there are so many carriers that they start to affect each other. One carrier falls into a trap and another carrier comes upon the trap but it's already filled! So it passes on by, without the delay of attempting to hop out of the trap. Thus, its transit time from contact to contact is decreased, and the overall velocity (corresponding to mobility) is increased. (By the way, the trapped carrier does eventually hop out again, but it is almost immediately filled by another carrier.)

As the charge concentration increases, the probability of carriers avoiding traps already filled increases, increasing the mobility and thus the conductivity. The quantity of injected carriers increases linearly with applied voltage; however the current no longer depends linearly

on the applied voltage. Instead, it obeys a power law: the current depends on voltage to the power of (m+1), where m is proportional to the characteristic energy of the distribution of traps[xxii]. Thus, the slope in the TLC regime can give clues as to the energy characteristics of traps within the device.

This power-law dependence of current on voltage will continue to higher voltages until all of the traps are filled, after which the I-V curve will either once again enter OC or SCLC.

Thus from the I-V characteristics it can be very clear in which regime the device is operating. In a log-log plot, the slopes vary from 1 to m* to 2 for OC, TLC, and SCLC, respectively. Much can be learned from examining the voltages at which a different regimes dominate operation of the device.

Interfacial Effects

There is one more piece of knowledge to discuss before we jump into the results: the most interesting aspect of our device is the interface parallel to the electric fields. What effect does an interface have on the optoelectrical behavior, if any at all? Not only does the interface provide a location for guaranteed dissociation of excitons but it also provides an optimal location for a conducting channel with an increased concentration of charge carriers.

It is much simpler to understand the behavior of the laterally-biased bilayer. Figure 15 shows the structure of a TPD/PTCBI device with interdigitated gold electrodes.

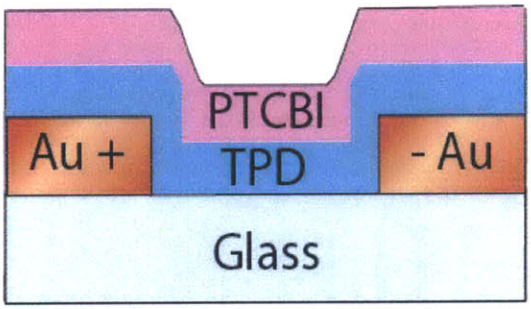

Figure 15 Diagram of the laterally-biased bilayer device. Most importantly, the TPD/PTCBI interface lies parallel to the applied electric field. As shown here, both organic layers are 50 nm thick and the electrodes are 70 nm high. The organic films are continuous over the full array of interdigitated gold electrodes of alternating applied voltage.

There are two aspects of effects of the interface on current through the device: on the generation of charge and on the transport of charge.

Charge generation at the interface

In our testing, PTCBI is utilized as the exciton generation layer (EGL). As excitons are generated in the bulk, they diffuse randomly, some finding the interface. At the TPD/PTCBI interface, an exciton will immediately dissociate into a hole in the TPD and an electron in the PTCBI (Figure 16). This mechanism can greatly increase the charge carrier concentration at the interface.

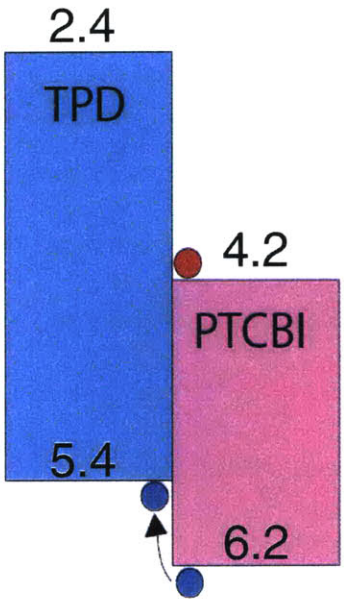

Figure 16 Dissociation of excitons at the TPD/PTCBI interface. The hole is swept to a TPD molecule as the electron remains on the PTCBI molecule. The two charges are then attracted to opposite contacts but may still recombine across the interface.

Transport of charge at the interface

As the carrier concentration at the interface increases, the conductivity in that region increases. This forms a conducting channel. This has multiple benefits: the charges generated from exciton dissociation and charges injected from the contact both add to the interfacial carrier concentration, pushing the device into the TLC regime at lower applied voltages. This leads to a much higher photocurrent.

However, an enhancement can be seen even in dark as shown in Figure 14. Due to the difference in energy between the two layers, carriers are swept across the interface to molecules with lower energy. This creates an accumulation of carriers on either side of the interface and thus a channel of higher conductivity.

Interfacial recombination

As we study the cartoon image of the dissociation of excitons at the interface, one thing is made clear: holes in the TPD may be merely a molecule away from electrons in PTCBI, and thus can quickly recombine. This effect can suddenly counteract the benefits of the interface. Data demonstrates that not every dissociated exciton instantly recombines, most likely since the electric field sweeps the charges apart before they recombine. However, the interfacial recombination rate increases as the concentration of photo-generated carriers increases: even if they are swept apart, the photo-generated carriers are likely to near other photo-generated charges and recombine.

This realization is somewhat discouraging: even though the interface can have great benefits, it is clearly under-utilized. Something more is needed.

C. Spacer Layers

A spacer layer is an interesting thing. From one view, it does nothing since it neither generates charge nor conducts charge. And yet, it can make all the difference in device behavior.

First, allow me to define a spacer layer. A spacer layer is an interfacial film that acts to separate two other layers. This covers anything and everything, but in this work I specifically study spacer layers that create a cascade-type energy structure, such as that described by Sista et al[xviii]. The benefit of cascade energy structures is that there are no energy barriers to the separation of charge carriers.

We chose to use Alq3 as the spacer layer in our laterally-biased trilayer. The interface between TPD and Alq3 has been studied in depth as a component of OLEDs, and the HOMO and LUMO energy levels of Alq3 fit within the HOMO and LUMO levels of TPD and PTCBI.

The device structure and energy structure are shown in Figure 17. Shown in Figure 17b are the film thicknesses, including a variable for the Alq3 thickness indicating the variation in thickness in experimentation.

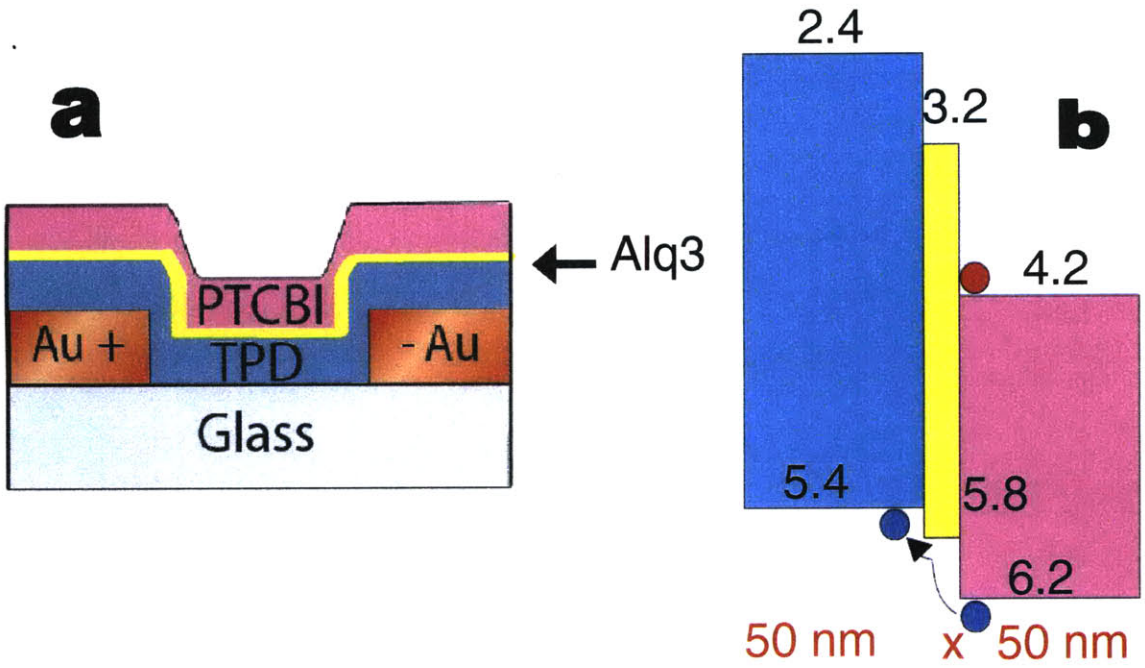

Figure 17 Diagrams of the laterally-biased heterojunction utilizing an Alq3 spacer layer. **a** The device structure showing the thin interfacial layer of Alq3. **b** The energy structure showing the cascade formed by the incorporation of Alq3. Both the TPD and PTCBI films are 50 nm thick, and the thickness of the Alq3 film is varied from 0 nm to 100 nm.

Effects of a spacer layer

The interface of PTCBI with Alq3 behaves just as the interface of PTCBI with TPD: an exciton dissociates into a hole and an electron. The electron stays in the PTCBI while the hole starts to drift towards the positive contact. However, there is also a drift in the vertical direction: as electrons build up at the Alq3/PTCBI interface the energy bands begin to bend and a field is

formed that pulls the holes away from the PTCBI. Also, simple diffusion provides a model for holes transporting through the Alq3. The photogenerated holes come upon the TPD/Alq3 interface and fall into the lower energy states of the TPD molecules. Thus, while in the bilayer the photo-generated carriers end up on either side of a single interface, in the trilayer the carriers have 2 interfaces and an entire film separating them.

Hence, the introduction of a spacer layer to the laterally-biased bilayer has two effects. Firstly, it distances the charges from each other, decreasing the attraction to recombine. Secondly, it forms an energetic barrier against their transport toward each other. Therefore the recombination rate can be drastically decreased and the device behavior enhanced. However, this is under the assumption that every photo-generated hole diffuses to a TPD molecule. If not, then the effect may be lost and the device current may even be diminished.

With these expectations and background in mind, we examine the behavior of the laterally-biased trilayer, especially in comparison with the bilayer device.

CHAPTER 4: DEVICE CHARACTERIZATION

Results from devices incorporating the Alq3 spacer layer have continually been both encouraging and discouraging. Although there has been large inconsistency (to be discussed at the bottom of this chapter), some trends have become evident. Shown below is one set of data that serves as an example of many others.

Characterization Methods for Optoelectronic Devices

Although multiple methods are available for characterizing the optoelectronic behavior of devices, I depend heavily on two: external quantum efficiency and current-voltage sweeps.

External Quantum Efficiency (QE) is a measure of a device's ability to convert light energy into electrical energy. Simply, it is the number of electrons out divided by the number of photons in. Experimentally, we expose the device to a lamp at a given wavelength and chopped with a given frequency and measure the photocurrent induced by the incident light (the current which is at that same frequency). From there, we calculate (with some complication) the photocurrent divided by the intensity of the incident light to determine the QE. An example external QE plot is shown in Figure 18 with the absorption spectrum overlaid. A peak in absorption corresponds to a peak in photocurrent and hence a peak in external QE.

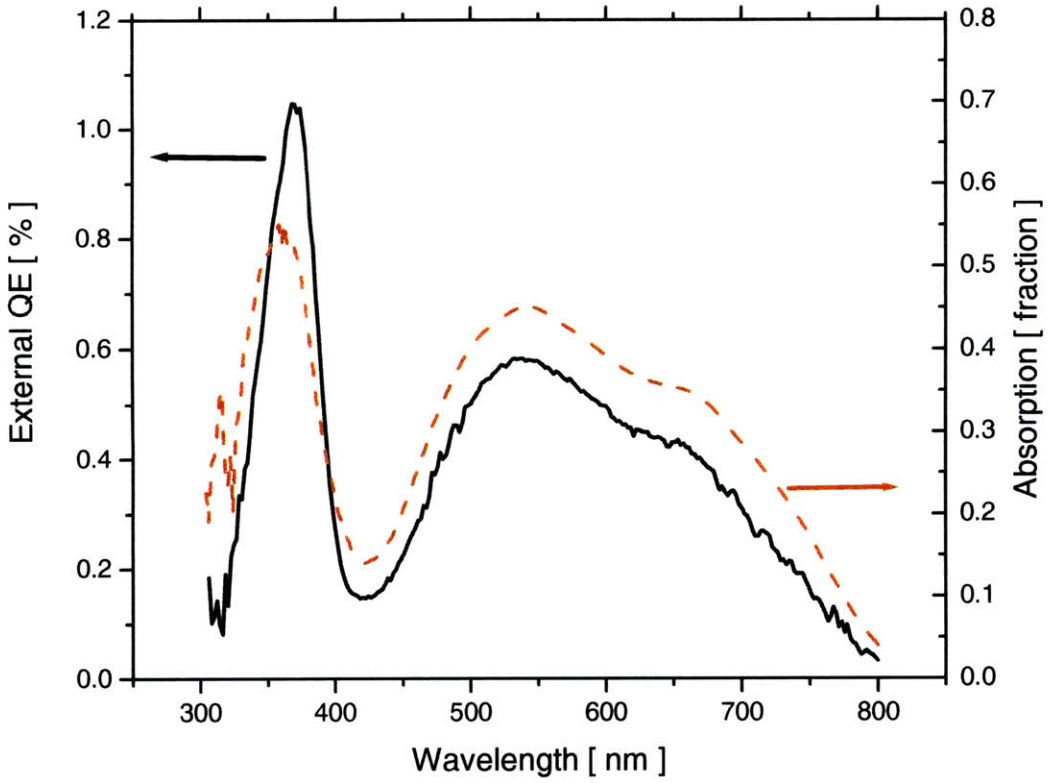

Figure 18 External QE Plot of a bilayer device overlaid with its absorption. The relationship between absorption and quantum efficiency is clear: peaks in light absorption correspond to peaks in external quantum efficiency.

Current-Voltage (I-V) sweeps give the electrical behavior of the device under different lighting conditions. Simply, we sweep the bias voltage from negative to positive and record the magnitude of the current. This is done both in dark and in light (the light exposure is from a green LED) so that the I-V characteristics can be compared and the photoresponse can be derived.

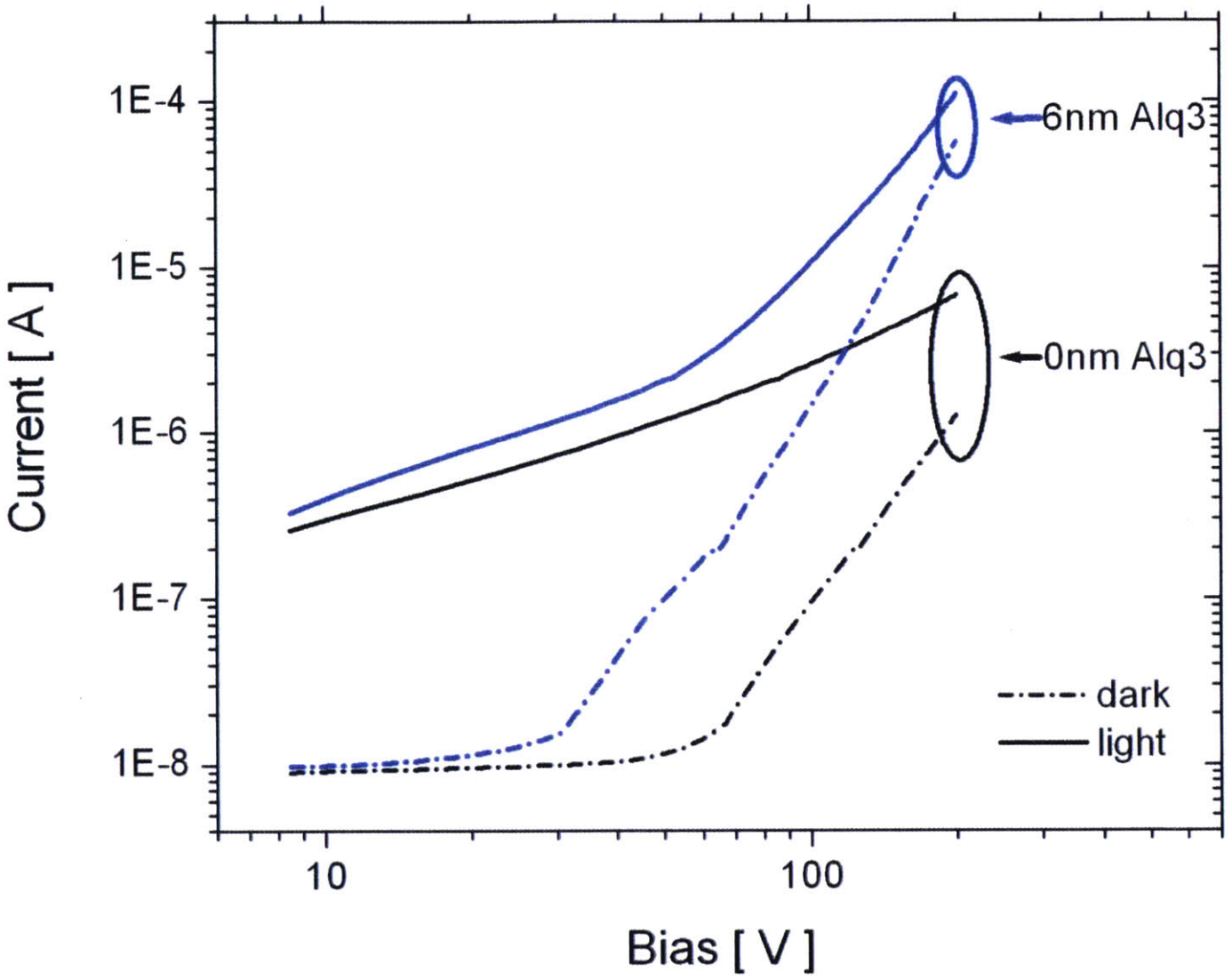

Figure 19

Figure 19 Current-Voltage Characteristics of a bilayer and trilayer device. The log-log plot shows transitions in both dark and light currents from Ohmic Conduction to Trap-Charge Limited Conduction, where the slope is greater than 2. Inset is a linear plot of the dark current "turn-on" with linear fits to the Ohmic Conduction regime.

Table 2: Summary of key values from Current-Voltage Characteristics

	Bilayer Device (0 nm Alq3)	Trilayer Device (6.2 nm Alq3)
Dark "Off" Slope	4.49E-11	9.42E-11
Dark Transition Bias	67	30
Dark TLC m*	3.28	3.76
		5.12
Light OC Slope	2.18	3.87
Light Transition Bias	50	~150

A. Conduction with no Light Excitation

Over the voltage range of -200V to 200V, there are two clear regimes in both the bilayer and trilayer: "Off" and Trap Limited Conduction (TLC).

"Off" Regime

At low bias voltages, the devices seem to be "off": have very low currents and very low conductivities. The devices may be either contact-limited or bulk-limited.

A contact limitation may be a Schottky barrier due to the difference in the HOMO of TPD (5.4 eV) and the workfunction of the gold contacts (5.2 eV). This difference in energies acts as a barrier to holes moving from the contact into the TPD. Schottky barriers give an exponential dependence of current on voltage, as at higher voltages the energy bands are bent more and it is more probable that holes will tunnel through the barrier.

It is unclear from the plot if the current is exponential at the transition or rather just an unsharp transition from two different power-laws. Also, it seems unlikely that such low electric fields such as those tested here (0.05 MV/cm) would create a large enough effect on the energy bands as to turn on a device that is limited by a Schottky barrier. (OLEDs are typically operated at electric fields of approximately 2 MV/cm[xix].) Since the barrier is undoubtedly there, it may be

that the charge concentration within the TPD is enough to bend the bands and minimize the barrier even at zero bias.

The presence of the Alq3 spacer layer decreases the voltage at which a transition occurs. If this transition is associated with overcoming the contact limitation, then that suggests that the Alq3 may be drastically increasing the charge concentration in TPD (either because of the interface or from doping) or somehow assisting in injection of holes (due to its high polarity and not favorable energies since the Alq3 HOMO is at 5.8 eV). Either of these would decrease the barrier to carrier injection and thus decrease the transition voltage.

The devices may instead/also be bulk-limited: the resistance of the organic films might be as high as to behave as an insulator. With insulators, the current is completely impeded until the breakdown voltage is reached, at which the material reaches a high enough temperature to give charge carriers enough energy to excite and conduct through the insulator. However, this mechanism is likely only if the device cools down faster than the time of a full run, since the dark current at both ends of the testing run exhibit the same "off" regime. The high resistance of these films is due to their low intrinsic charge concentrations and the difficulty of charge hopping from molecule to molecule, especially with the presence of traps.

A complication is that the range of the "off" regime is highly dependent on testing parameters, especially length of time for each measurement. This may further corroborate the bulk-limited theory. If the measurements are slow enough, then the device has time to increase charge concentration to the steady-state and fill traps, thus increasing conductivity. However the measurements—even at their fastest—are on the order of hundreds of milliseconds, suggesting a ridiculously long time response (which, actually, we do see during testing). This time-dependence deserves further study.

TLC Regime

In the trap-limited conduction (TLC) regime, both the trilayer and the bilayer have m*[5] approximately equal to 3.5 (3.38 and 3.76 decade/decade, respectively). m* depends on the energetic distribution of the traps within a semiconductor such that m* = 3.5 gives T_c = 750K at T = 300K. This is a relatively small value for T_c, so the trap distribution is narrow[xx]. Literature suggests that TPD has a very narrow trap distribution[xxi], so this may show that conduction is through the TPD bulk rather than at the interface where there would be a broader distribution. Another possible explanation for the low m* is that this regime is still within the transition between SCLC and TLC. Conduction could be occurring through both the bulk TPD (SCLC, m* = 2) and the interface between TPD and the film above it (TCL, m* = unknown). Further research of this possible mechanism is discussed in Chapter 6.C.

The trilayer has a second transition to a slope of 5.12 decades/decade at approximately 100V. The data is unclear as to whether the control would also reach this transition at a higher voltage. (Higher bias than 200V increases the rate of degradation due to operation, and thus it is avoided.) However, the exhibition of this transition only in the trilayer suggests that the presence of the spacer layer either drastically increases the carrier concentration or changes the trap distribution in the conducting channel.

At no point within the operating voltages does the trilayer device exhibit m* similar to that demonstrated in Shen et al. (7±1 at 300 K)[xxii] for TLC through Alq3, and thus conduction in the trilayer device is not dominated by the bulk of the Alq3 spacer layer.

[5] m* is the slope of the log(I)-log(V) plot. Recall that m* is a representation of the expressions (m+1) and (n+1) found in literature[xxii,xx].

B. Conduction with PTCBI Photoexcitation

When exposed to a green LED, the magnitude of the current is several magnitudes higher than in the dark. This current is the light current and is most simply analyzed as the superposition of the dark current and the photocurrent. (This approximation holds for light current much greater than the dark current). Both multilayer photoconductors turn on their light current even at very low voltages and operate in OC until transitioning to TLC at high voltages.

OC Regime

At low voltages, the device operates in OC, where m* is approximately equal to 1 (as in a conventional resistor). The device still operates in an OC regime in light even though while the dark current operated with TLC at the higher voltages. Presumably, the light current has a far higher concentration of charge carriers than the dark current due to the presence of photogenerated carriers. We can explain the existence of an OC regime at low voltages in light by proposing that at low voltages, the charge carrier concentration is changing insignificantly with bias as compared to the photogenerated carrier concentration. As such, a small increase in voltage will not effect the carrier mobililties (which is the cause of $m^* > 2$ in TLC) and thus the device will operate in OC ($m^* \approx 1$).

In the OC regime, the slope of the light current is linearly dependent on the conductivity of the device. We see that the slope of the trilayer is roughly twice that of the bilayer (3.87 and 2.18 Ω, respectively), suggesting that the charge carrier concentration in the conducting channel is doubled with the presence of the Alq3 spacer layer. The carrier concentration is the only parameter that would change since such a small change in concentration would not change the carrier mobility significantly. This again suggests that the presence of the Alq3 spacer layer increases the free charge carrier concentration, but this calculation is complicated by the fact that

many carriers are trapped and the trap distribution may or may not change with the introduction of the Alq3 spacer layer. Whatever the mechanism, it is clear that the presence of a spacer layer increases the device's conductance in light.

TLC Regime

At higher biases, the devices begin to transition to TLC, however device operation does not completely transition to TLC within the voltage range applied to either device. Once again, the trilayer transitions at lower voltages than the bilayer device. This may occur through the same mechanisms as suggested above for device operation in dark: either the Fermi level of the trilayer device is in a different position in its trap distribution or the presence of the spacer layer causes a greater dependence of carrier concentration on bias.

Since neither device fully operates in TLC at the highest applied voltages, we are unable to characterize and compare the behavior of the devices in light with the behavior in dark.

C. Photoconduction

QE data for a series of Alq3 thickness are shown in Figure 20. An enhancement factor (behavior of the trilayer divided by behavior of the bilayer) of 10 is demonstrated with the interfacial incorporation of 6.2 nm of Alq3. As the thickness of the spacer layer increased, the effect on QE also increased from doubling the QE at a barely continuous film nominally 2 nm thick to an order of magnitude improvement with an Alq3 film 6 nm thick, or roughly 6 molecular layers. However, there is a sharp drop off in QE with 8.2 nm thick Alq3 layer, such that it is roughly the same QE as that of the control (0nm Alq3).

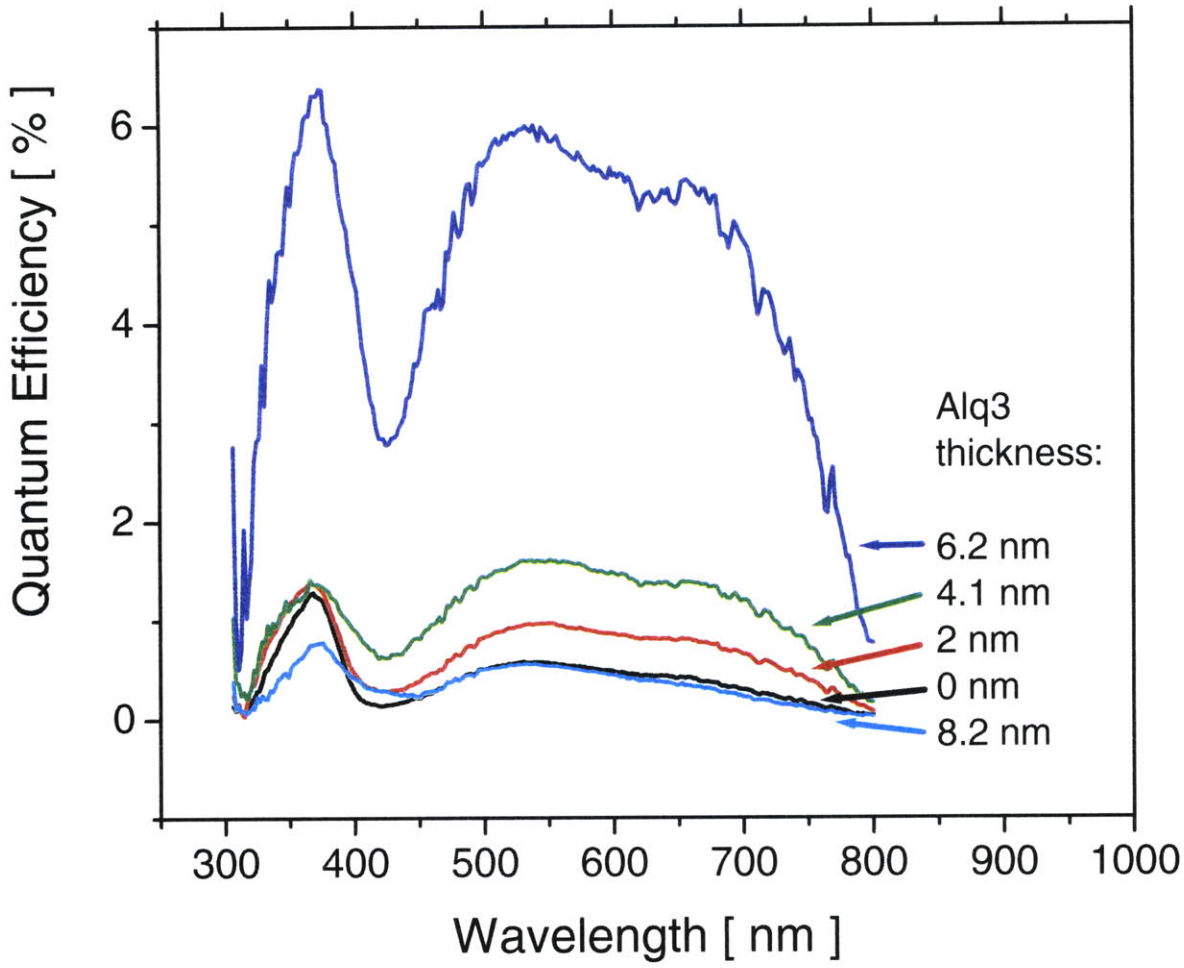

Figure 20 Plot of Quantum Efficiency over the visible spectrum for devices with varying thicknesses of Alq3. Both the TPD layer and the PTCBI layer were 50 nm for all devices. The figure clearly shows an order of magnitude increase in QE from the bilayer device (0 nm) to the best trilayer device (6.2 nm Alq3 thickness) at the PTCBI absorption peak (539 nm).

Enhancement

The enhancement in QE with the introduction of an Alq3 spacer layer can be caused by multiple mechanisms.

Summarily, the spacer layer may increase the conductivity in dark by changing a contact barrier, by increasing carrier concentrations in the device or by changing the trap distribution. These mechanisms and their potential are discussed above.

The potential mechanism of interest is that the spacer layer may decrease the recombination rate across the interface by distancing the photogenerated carriers. The impact of this mechanism depends highly on the magnitude of the interfacial recombination rate, which is dependent on the concentration of excitons at the interface. It would affect the dark current insignificantly if there is a negligible interfacial recombination rate in steady-state. However, this would have a significant effect at high concentrations of excitons. The effect of exciton concentration is currently being studied; see Section 6.E for discussion on further research to explore this effect.

Whatever the mechanism, the data shows clearly that the utilization of the Alq3 spacer layer can drastically enhance the QE. However, this enhancement is strongly dependent on the thickness of the Alq3 film.

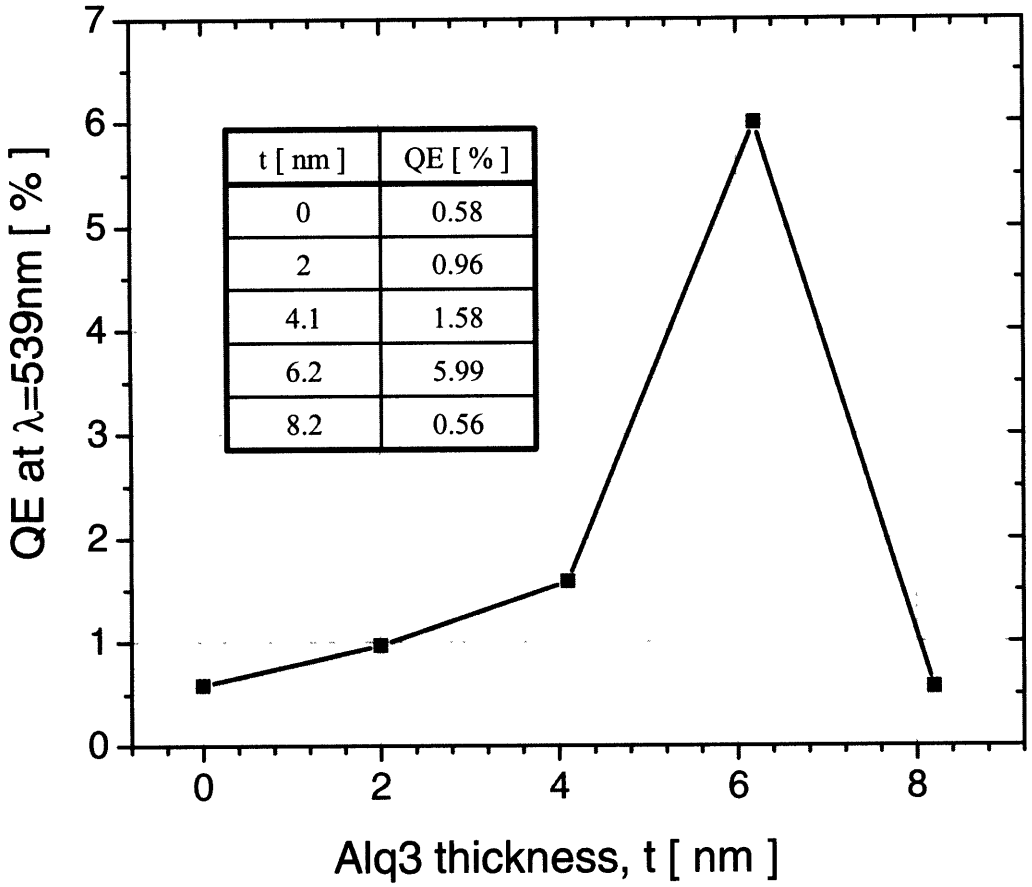

Figure 21 Dependence of Quantum Efficiency on Alq3 Thickness. A clear trend of increasing thickness to increasing Q.E. at the PTCBI absorption peak is demonstrated, with an order of magnitude enhancement at the optimal Alq3 thickness of 6.2 nm.

Thickness Dependence

The QE of the devices at the PTCBI peak absorption wavelength increases slightly at 2 and 4 nm of Alq3, increases dramatically at 6nm and decreases dramatically at 8 nm. The increase at 6 nm may depend on the transition from OC to TCL, whereas the decrease at 8nm may depend on the low conductivity of hole transport through the Alq3 film.

Firstly, we examine the increase at small thicknesses. QE is measured at 90V: right in the transition region between OC and TCL as seen in the I-V curves. For the devices operating in the OC regime at 90V, the QE has a simple linear dependence on thickness due to the slight increases in charge concentration at the interface. This may be due to intrinsic changes in the device with varying Alq3 thickness or due to decreasing the interfacial recombination rate.

At 90V with photoexcitation, the bilayer hasn't yet transitioned to TCL and still operates in the OC regime, but the trilayer with 6.2 nm Alq3 operates in the TCL and thus has higher currents. This explains the dramatic increase in enhancement for an Alq3 film thickness of 6.2 nm. Possible reasons for the difference in transition voltages are discussed above.

But what about dramatic decrease in QE for the device with an 8.2 nm thick film of Alq3? I-V characteristics for 8.2 nm Alq3 show that the device turns on at a higher bias than any of the trilayer devices with thinner spacer layers. This gives two possible answers: either the thickness of the Alq3 film increases the contact barrier or the bulk of the Alq3 film begins to drastically affect the photocurrent at a thickness of approx. 8nm.

One possible reason for a decrease in QE at thicker Alq3 films is that the Alq3 film has a very low conductivity for holes and that inhibits hole transport from the EGL to the CTL. The conductance of the film is inversely proportional to distance (assuming that the carrier travels perpendicular to the interface). However it's possible that carriers tunnel through the spacer layer at smaller thickness but are less able to do so at larger thicknesses.

Another possible reason for the dramatic decrease is hole transport is a known mechanism for Alq3 degradation[xxiii] and that is exactly its use in this device. For thicker films, there is more hole transport and perhaps a higher likelihood for degradation. Larger thicknesses

of Alq3 should be studied to determine the continuing dependence of QE on spacer layer thickness.

D. Consistency Issues

However, these results are not consistent across devices. Often the controls themselves can vary widely in their behavior, and trilayer devices of the same thickness can have different enhancements (or, more often, diminishments). This likely is paradigm of one of the greatest disadvantages of organics: degradation. Organic materials can degrade quickly, especially in the presence of oxygen or moisture (and especially the TPD film, used as the CTL). Beyond that, these films are very particular about their growth parameters: changing the temperature of the source or substrate during growth, changing the growth pressure, changing even the distance of a substrate from a source can have vast impacts on the morphology of the organic film.

The mechanisms of inconsistency are currently being investigated. See the Section 6.A and 6.B for suggestions of methods of studying the differences between devices: the possibility of mixing at the interface.

CHAPTER 5: CONCLUSIONS

This thesis demonstrates the enhancement of organic multilayer photoconductors through the utilization of a spacer layer. As shown in Chapter 4, trilayer photoconductors exhibit an order of magnitude enhancement over bilayer photoconductors. The enhancement had a strong dependence on the thickness of the spacer layer, with a maximum enhancement of photocurrent (as displayed in Q.E.) for devices with an Alq3 film thickness of approximately 6 nm.

There are many factors influencing the photocurrent, and thus this enhancement may or may not correspond with a reduction in recombination rate. Other factors include differences in trap distributions at the interfaces and increased charge concentration at the interface due to doping by Alq3. Determination of which of these factors exist and dominate requires further experimentation (see Chapter 6).

This thesis work suggests that the utilization of a spacer layer within the lateral multilayer photoconductor can have dramatic effects on the performance of a chemosensor fabricated with the same device structure. An order of magnitude enhancement in photocurrent as demonstrated in this work would correspond with a significant increase in sensitivity. As development of a multilayer photoconductor comprising of a sensing polymer continues, this work gives evidence for the utilization of a spacer layer.

CHAPTER 6: FUTURE WORK

A. Annealing

Temperature can have amazing effects on devices. There is paper after paper demonstrating the effects of temperature on operation of devices, both temporarily during operation (affecting the energy of electrons and the broadness of energy states) and in the long-term by changing the morphology and interfacial structure. Especially with organic films (which have very low transition temperatures), high temperatures introduced by device operation can quickly degrade devices. This has led to an enormous amount of research in the OLED field.

The wondrous effects of temperature have also been used through annealing as a technique to affect devices before operation. (some example from inorganics). Peumans et al[xxiv] annealed mixed-layers of organics to form bulk heterojunctions that led to enhancement in organic solar cells. We recommend future work on the effects of annealing on the optoelectrical behavior of organic multilayer photoconductors.

Preliminary results are shown in Figure 22. It is clear that ten minutes annealing at 100oC can have dramatic effects on the performance of a device and that the effect is dependent on the presence and thickness of an Alq3 spacer layer. The mechanisms of this improvement are currently being investigated.

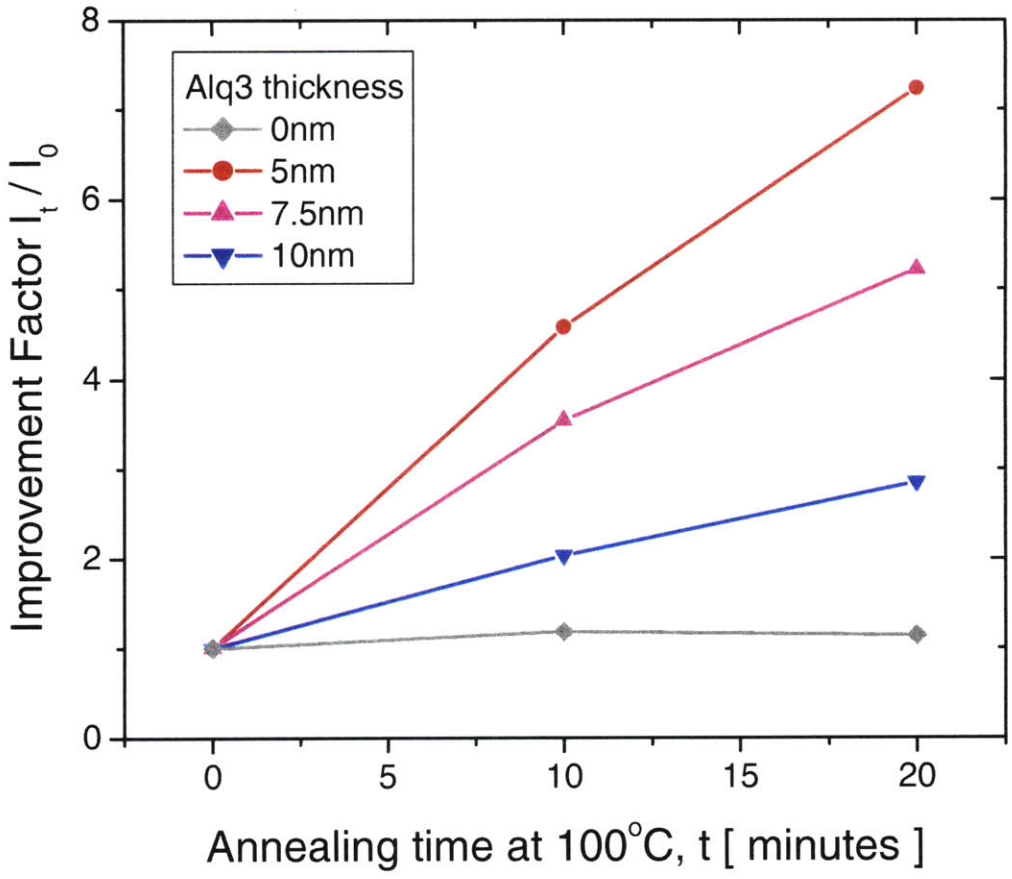

Figure 22 Effects of Annealing on the Light Current of Organic Multilayer Photoconductors.

B. Interfacial Studies

One possible factor influencing enhancement is the interface: doping of TPD and/or PTCBI by Alq3, or changes in the trap distribution at the interface. It is important to examine these effects.

Mixing of the Alq3 into PTCBI and/or TPD can possibly be imaged via cutting through FIB and examination via AFM. And the possible effects of mixing can be studied through depositing mixed layers at the interfaces and comparing optoelectrical behavior of the mixed devices with that of the devices characterized here.

The trap distribution in the trilayer can be further understood through further examination of the current-voltage characteristics and through temperature studies.

C. Existence of a Conduction Channel

The theoretical model for the behavior of both the bilayer and trilayer devices includes the existence of a conduction channel. In the CTL within a certain distance of the top interface, photogenerated carriers may accumulate. The high carrier concentration creates a channel with much higher conductivity than the bulk, and thus conduction will occur through this conduction channel. To examine the reality of this model we can vary the thickness of the CTL to determine if very thin devices are entirely conductive in the bulk whereas very thick devices transition to conduction through a small channel.

D. Further Materials

If reducing the recombination rate by spacing the charges is truly the mechanism behind the enhancement of photocurrent, then the enhancement should be repeatable with a different material used as a spacer layer but also forming a cascading energy structure. One potential material is CBP, which also forms a cascading energy structure when utilized as a spacer layer. It is very important to prove that enhancement depends on the existence of a spacer layer rather than the presence of Alq3 at the interface.

Also, we can examine the ability of a wide-band gap spacer layer to entirely inhibit the photocurrent. A material such as BCP would block excitons from splitting at the interface and prevent photogenerated carriers from transporting to the CTL. This should produce a light current equal to that of the dark current.

E. Dependence on Interfacial Recombination Rate

The impact of the spacer layer is greatly dependent on the magnitude of the interfacial recombination rate: if interfacial recombination is non-existent, then the spacer layer will offer no enhancement of the photocurrent. Thus, a method to further explore the impact of the spacer layer is to vary the interfacial recombination rate. This may be performed by varying the light intensity in testing: as the device is exposed to higher intensities of light, there will be higher concentrations of excitons and thus higher concentrations of photogenerated carriers at the interface. Recombination rate is dependent on concentration and so it will also increase. Large recombination rates allow us to examine the impact of the spacer layer more clearly. Such experimentation is currently being performed.

CHAPTER 7: WORKS CITED

[i] "MIT gel changes color on demand". *MIT Tech Talk.* Oct. 2007. http://web.mit.edu/newsoffice/2007/lightgels-1021.html

[ii] "MIT gas sensor is tiny, quick". *MIT Tech Talk.* Jan 2008. http://web.mit.edu/newsoffice/2008/micro-analyzer-0110.html

[iii] Yang, Jye-Shane and Timothy M. Swager. "Porous Shape Persistent Fluorescent Polymer Films: An Approach to TNT Sensory Materials". *J. Am Chem. Soc.* **120**. 1998

[iv] Zaretsky, Mark C., James R. Melcher, and Chathan M. Cooke. "Moisture Sensing in Transformer Oil using Thin-film Microdielectrometry". *IEEE Transactions on Electrical Insulation*, **24**, No. 6. 1989.

[v] Van Gerwen, Peter, et al. "Nanoscaled Interdigitated Electrode Arrays for Biochemical Sensors". *Transducers*. 1997.

[vi] Miasik, Jan J., Alan Hooper and Bruce C. Tofield. "Conducting Polymer Gas Sensors". *J. Chem. Soc, Faraday Trans. 1*. **82**. 86.

[vii] Ho, J. Arango, A. and V. Bulovic. "Lateral Organic Bi-layer Heterojunction Photoconductors". *Appl. Phys. Lett.* In publication.

[viii] Pope, M and C. Swenberg. *Electronic Processes in organic crystals*. Oxford Univ. Press. 1982.

[ix] Naka, S. et al. "Carrier transport properties of organic materials for EL device operation." *Synthetic Metals*. **111-112**. 2000.

[x] Pierret, R. *Semiconductor Device Fundamentals*. Addison Wesley. 1996.

[xi] Rand, B. "Mixed donor-acceptor molecular heterojunctions for photovoltaic applications. I. Molecular properties." *J. App. Phys.* **98**. 2005.

[xii] Kepler, R. G., et al. "Electron and hole mobility in tris(8-hydroxyquinolinolato-N1,O8) aluminum". *Appl. Phys. Lett.* 1995.

[xiii] Tang, C.W. and S. A. VanSlyke. "Organic electroluminescent diodes". *Appl. Phys. Lett.* **51**.1987.

[xiv] Szmytkowski, J. et al. "Electric field-assisted dissociation of singlet excitons in tris-(8-hydroxyquinolinato) aluminum (III)". *Appl. Phys. Lett.* **80**, no. 8. 2002.

[xv] Madigan, C. F. "Theory and Simulation of Amorphous Organic Electronic Devices". MIT PhD Thesis. 2006.

[xvi] Shimakawa, K. et al. "Photo-carrier transport in disordered organic TPD films". *J. Non-Crystalline Solids*. **352**. 2006.

[xvii] Forrest, S.R., Kaplan, M.L., and P.H. Schmidt. "Organic-on-inorganic semiconductor contact barrier diodes I. Theory with applications to organic thin films and prototype devices". *J. App. Phys.* **55.** 1984.

[xviii] Sista, S. et al. "Enhancement of open circuit voltage through a cascade-type energy band structure". *J. App. Phys.* **91**. 2007.

[xix] Burrows, P. E. et al. "Reliability and degradation in organic light emitting devices". *J. App. Phys.* **65.** 1994.

[xx] Rose, A. "Space-Charge-Limited Currents in Solids". *Phys. Rev.* **97**, no. 6. 1954.

[xxi] Karg, S., Steiger, J. and H von Seggern. "Determination of trap energies in Alq3 and TPD". *Synthetic Metals* 111-112. 2000.

[xxii] Shen, Z. et al. "Temperature Dependence of Current Transport and Electroluminescence in Vacuum Deposited Organic Light Emitting Devices". *Jpn. J. Appl. Phys.* **35.** 1996.

[xxiii] Popovic, Z. et al. "Simultaneous electroluminescence and photoluminescence aging studies of tris(8-hydroxyquinoline) aluminum-based organic light-emitting devices". *J. Appl. Phys.* **89**, no. 8. 2001.

[xxiv] Peumans, P., Uchida, S., and S. Forrest. "Efficient bulk heterojunction photovoltaic cells using small-molecular-weight organic thin films". *Nature*. **425**. 2003